Electronic Supplementary Material (ESI) for Journal of Materials Chemistry A.

Supplementary data

Promoted Interfacial H_2O Supply by Surface Hydroxyl Groups for Enhanced Alkaline Hydrogen Evolution

Lejuan Cai, Ziyuan Lin, Mengye Wang, Feng Pan, Jiewei Chen, Yi Wang, Xinpeng Shen, Yang Chai*

Department of Applied Physics, The Hong Kong Polytechnic University, Hung Hom, Kowloon, Hong Kong, People's Republic of China

*To whom the correspondence should be addressed: y.chai@polyu.edu.hk

Experimental section

Synthesis and Preparation: The MoS_2/3D graphene structure synthesis was composed by two steps. At first, 0.1 g glucose, 0.1 g $(NH_4)_2MoS_4$ and 1.0 g NH_4Cl were dispersed in 20 mL ethanol by vigorous stirring to uniformly coat the glucose and $(NH_4)_2MoS_4$ on the surface of NH_4Cl. Next, the mixture was then baked on a hot plate at 65 °C under a continuous stirring to vapor the solvent. After ethanol evaporation, grey black precursors can be collected. The grey black precursors then experienced a two-step annealing process in a tube furnace, the heating rate was 10 °C /min. The heating center temperature of the furnace was raised up to 500 °C and held at this temperature for 60 min, and was then continuous raised the temperature to 1000 °C in 100 min, followed by a constant reaction temperature of 1000 °C for 30 min. H_2 atmospheres was selected in the first-stage of annealing process to lower the decomposition temperature of $(NH_4)_2MoS_4$ and increase the content of sp^3 carbon in graphene frameworks. The second annealing was performed under Ar atmosphere, accounting for the etching interaction between H_2 and MoS_2 when the temperature was above 500 ℃. Other M/3D graphene structures (M = Pt, Fe, Ni@NiO or Co@CoO) were fabricated via above annealing process except for replacing the 0.1 g $(NH_4)_2MoS_4$ with 0.021 g $H_2PtCl_6•6H_2O$, 0.062 g $FeCl_3$, 0.112 g $Ni(NO_3)_2•6H_2O$ or 0.095 g $Co(CH_3COO)_2•4H_2O$, respectively. The M/3D graphene structures (M = Pt, Fe, Ni@NiO or Co@CoO) were denoted as Pt-G, Fe-G, Ni@NiO-G or Co@CoO-G, respectively. The hydroxylated samples were obtained by treating the samples in a 1.0 M NaOH solution, then the dispersed samples in the NaOH solution was washed with DI H_2O.

Electrochemical Tests: A three electrodes electrochemical station was used to perform electrochemical measurements (Solartron Analytical). All alkaline tests were performed in a solution of 50 mL of 1.0 M NaOH electrolyte (pH = 14.0), the HER performances in neutral medium was performed in 0.5 M Na_2SO_4. Typically, 10 mg of sample and 20 µL Nafion solution were dispersed in 1.0 mL isopropanol solution, followed by ultrasonic treatment for 1 h to form a homogeneous ink. Then 10 µL of the dispersion was loaded onto a polished glassy carbon electrode with the diameter of 3 mm. The glassy carbon electrode loaded with sample, graphite rod and Hg/HgO were applied as working electrode, counter electrode and reference electrode, respectively. The performance of the HER was tested using linear sweep voltammetry (LSV) with a scanning window of 0 V to -0.8 V vs RHE and a scan rate of 10 mV s^{-1}. The durability of MoS_2-G was evaluated by cycling test of 3000 times. All the LSV curves are corrected with iR compensation.

Electrochemical active surface area: Electrochemical capacitance measurements were used to calculate the active surface area of the MoS_2-G. The applied potential was set between 0.12 to 0.22 V vs. SCE for 20 cycles at different scan rates (5, 10, 20, 30 and 50 mV/s). The capacitive currents were measured in the potential range of no faradic reactions and the current data were collected at the 0.17 V vs. SCE. Then, the capacitive currents were plotted as a function of scan rate to calculate the double layer capacitance. The EASA can be calculated based on following equation:

$$\text{EASA}=C_{dl}/C_s$$

C_{dl} is the double layer capacitance and C_s is the specific capacitance. In general, the specific capacitance for a flat surface is in the range of 0.02-0.06 mF/cm^2. In this paper, we choose the value of 0.04 mF/cm^2 in 1.0 M NaOH to calculate the EASA.

Characterizations: The morphology of MoS_2/3D graphene structure was characterized by scanning electron microscope and scanning transmission electron microscope (SEM, Jeol JSM-6335F & TEM, Jeol JEM-2100F). The crystal structure and composition of MoS_2/3D graphene structure were measured by X-ray Diffractometer (Rigaku SmartLab) and Raman spectroscope (Horiba HR800) with an excitation wavelength of 488 nm. The electrochemical impedance spectroscopy (EIS) of MoS_2-G before and after alkaline treatment were performed by a three-electrode configuration using CHI-660E electrochemical analyser. The surface valence state of samples were tested by using X-ray photoelectron spectroscopy (XPS, Thermol Scientific Escalab 250Xi, Al Kα radiation). The contact angle of samples were investigated by water contact angle measurement (SDC-350).

Theoretical Calculations: Theoretical calculations were performed using density functional theory (DFT) as implemented in the VASP code (5.4) with exchange-correlation energy functional, which were modeled by Perdew-Burke-Ernzerhof (PBE) functional.[1] The cut-off energy was set to be 450 eV and all structures were relaxed to an energy convergence of 10^{-5} eV/atom and a force convergence of 0.02 eV/Å, respectively. During the geometrical optimization, 2 × 2 supercell was applied to mimic the H_2O adsorption on graphene and the k-points was 3 × 3 × 1. The thickness of vacuum in all the models was set to 30 Å to eliminate the interactions between the layers caused by the periodic boundary condition. Van der Waals (vdW) interaction correction was applied to all the structures by Grimme's DFT-D2 method.[2] The adsorption energy of adsorbed H_2O, E_{ad}, was defined as the mean adsorption energy per H_2O molecule of the structure:[3]

$$E_{ad} = (E_{(H_2O)/sub} - E_{sub} - n\times E_{H_2O})/n$$

The binding energy of free H_2O cluster, E_{bind}, was defined as the mean binding energy per H_2O molecule of the structure:

$$E_{bind} = (E_{cluster} - n\times E_{H_2O})/n$$

Here, $E_{(H_2O)/sub}$ is the total energy of the adsorption system, E_{sub}, $E_{cluster}$ and E_{H_2O} are energies of the substrate, free H_2O clusters and free molecules, respectively, and n is the number of H_2O molecules in the supercell.

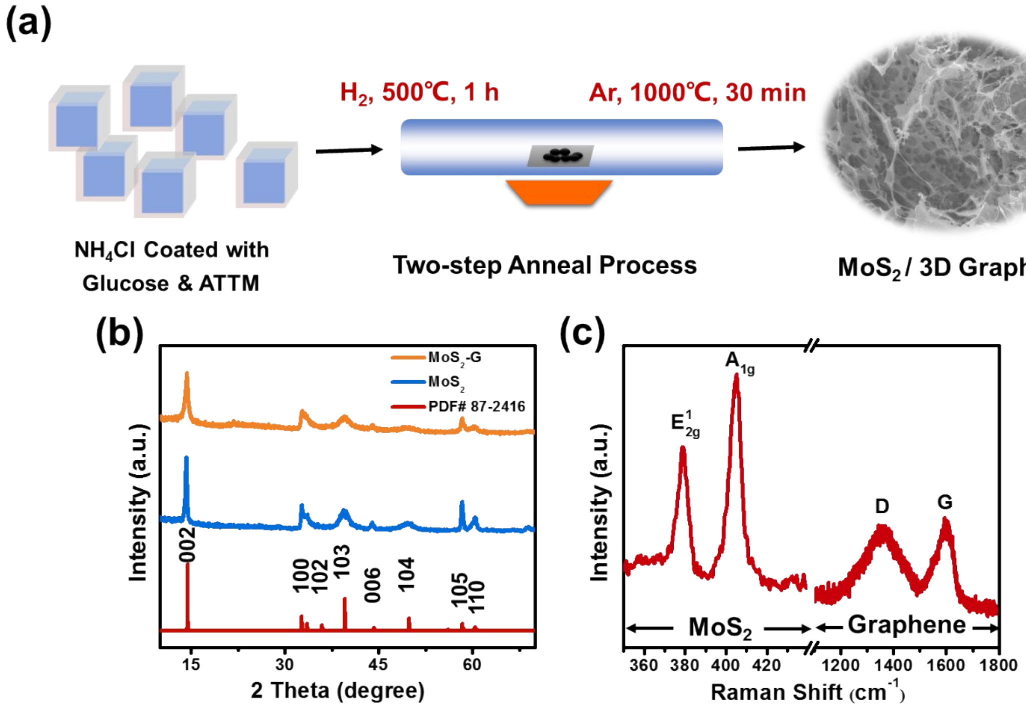

Figure S1. (a) Schematic illustration of the two-step thermolysis process for the fabrication of porous MoS_2-G structure. (b) X-ray diffraction spectra of the as-grown porous MoS_2-G and MoS_2 nanosheets prepared under the same anneal process. (c) Raman spectra of the porous MoS_2-G sample.

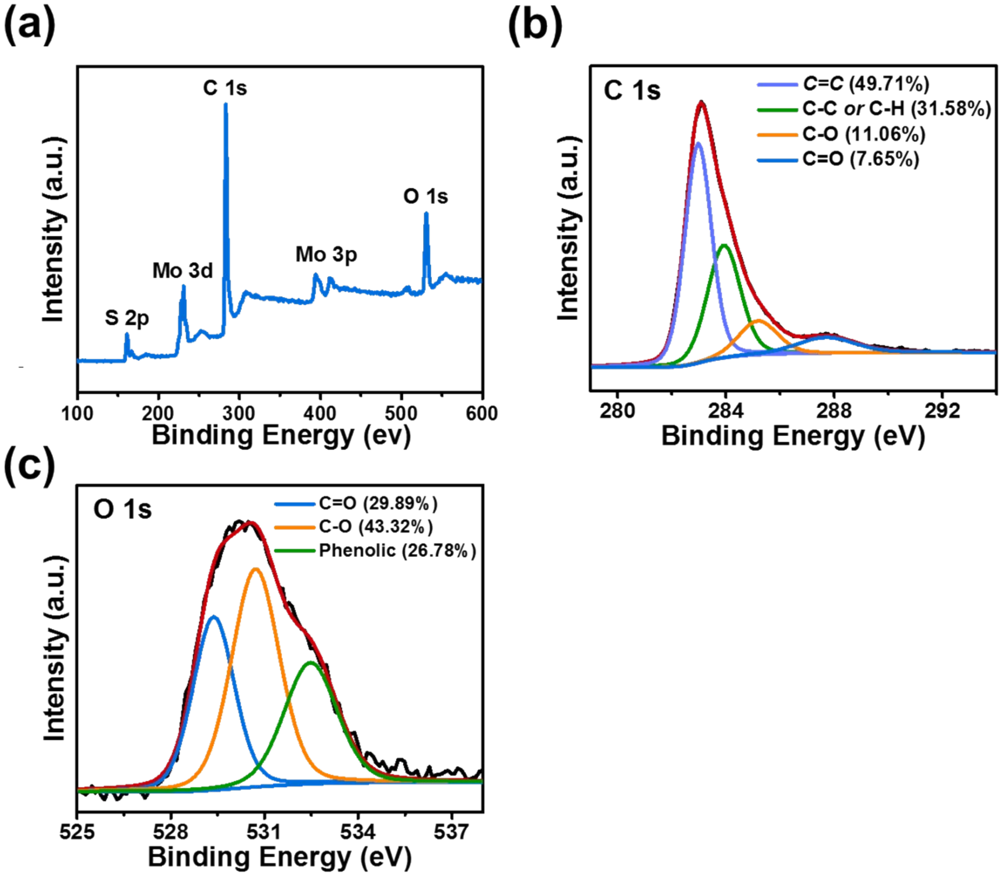

Figure S2. (a) XPS spectra of prepared MoS_2-G. (b) The C1s and (c) O1s XPS spectra of MoS_2-G sample.

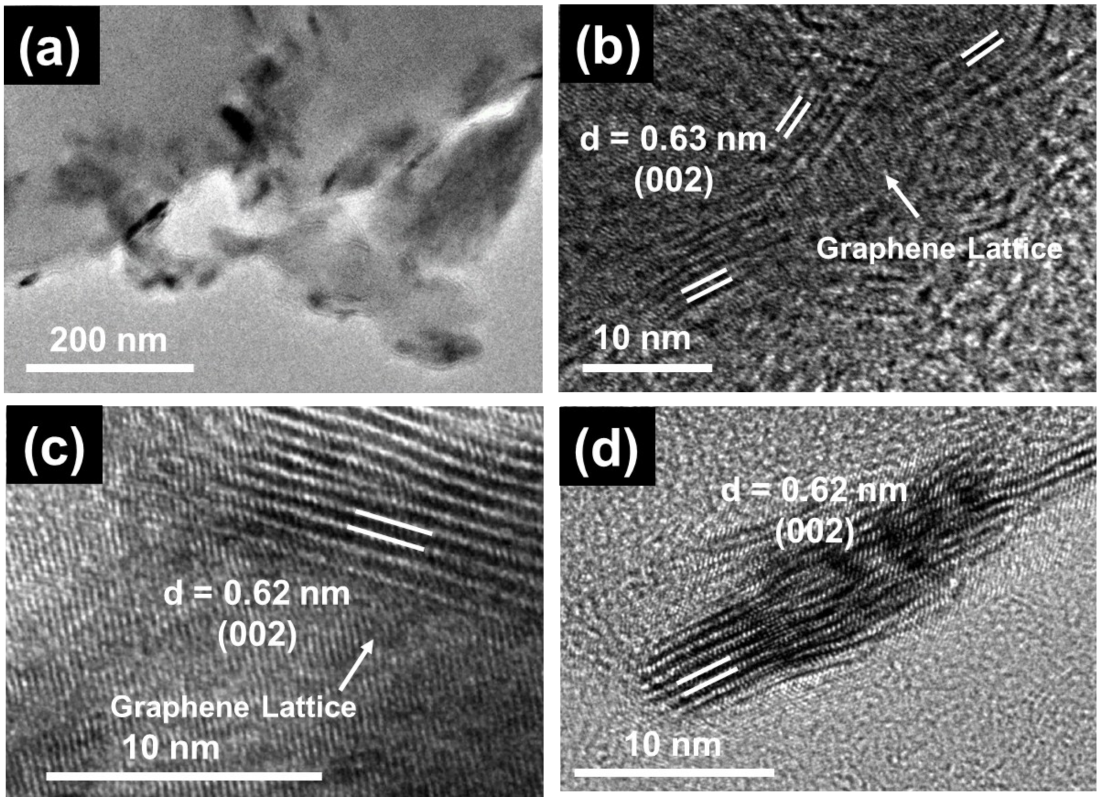

Figure S3. (a) TEM and (b-d) HRTEM images of the MoS_2-G heterojunctions.

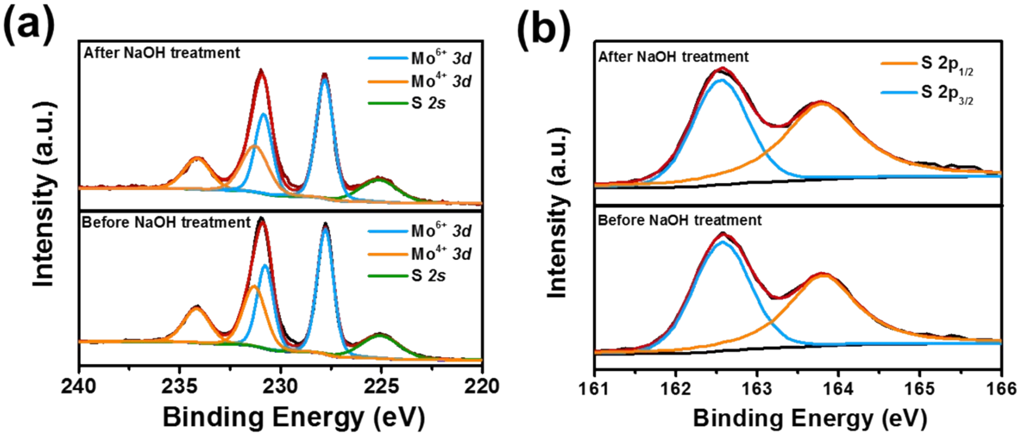

Figure S4. Chemical composition analysis by XPS for (a) Mo and (b) S in MoS_2-G sample before (downside) and after NaOH treatment (upside).

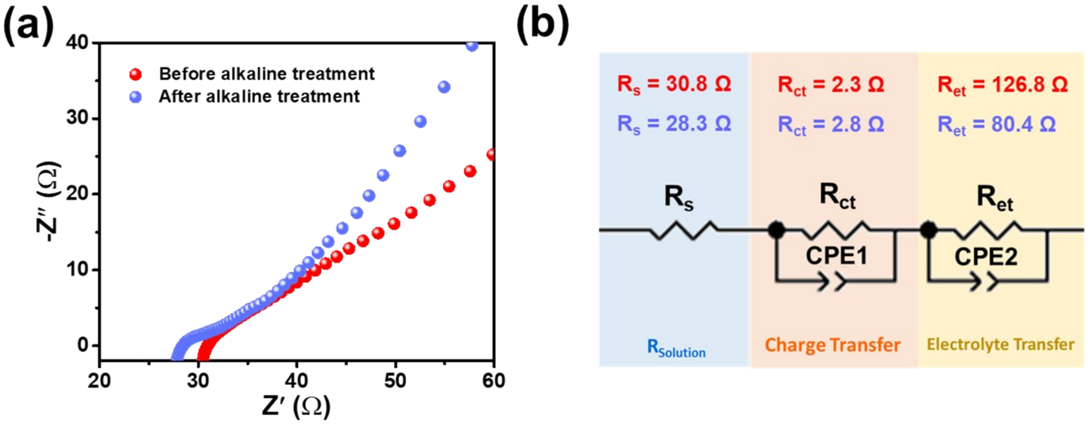

Figure S5. (a) The electrochemical impedance spectrum of MoS_2-G before and after alkaline treatment. (b) The equivalent circuit for EIS fitting.

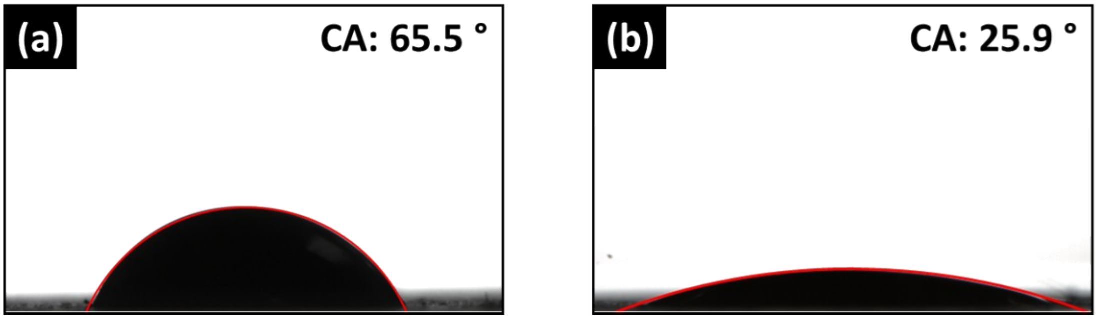

Figure S6. Contact angles of MoS_2-G (a) before and (b) after alkaline treatment.

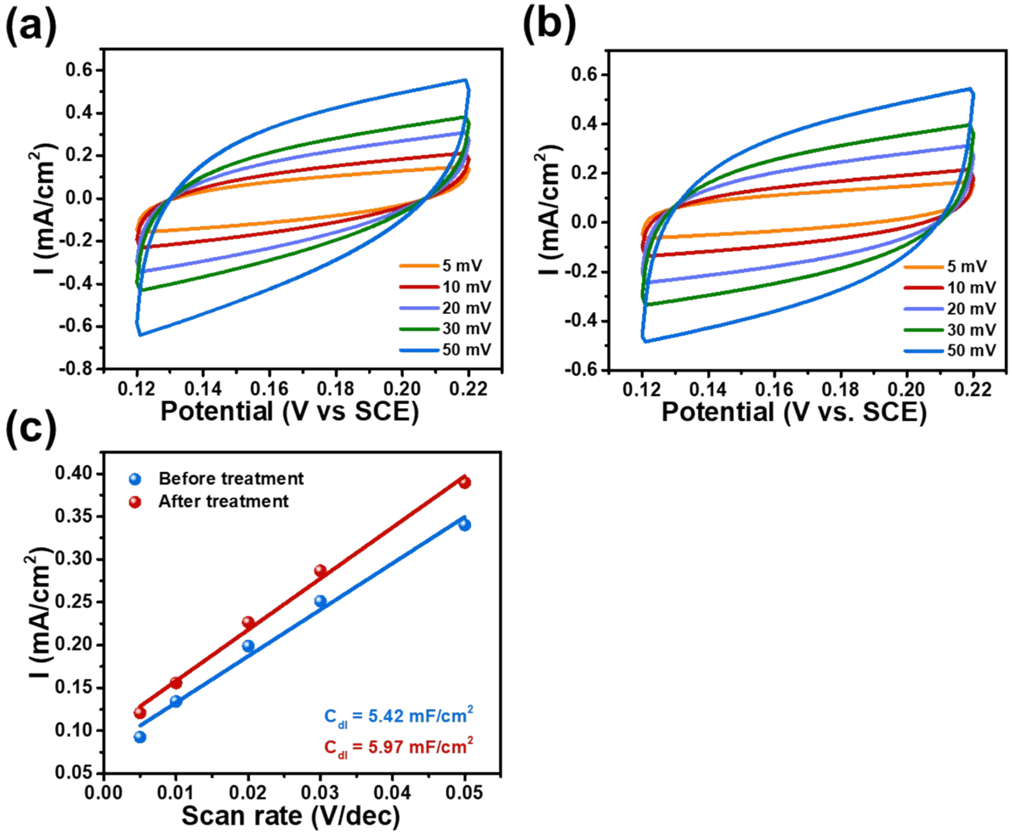

Figure S7. Cyclic voltammograms were tested in the non-faradaic region of 0.12–0.22 V of MoS_2-G (a) before and (b) after alkaline treatment. (c) Polarization curves of MoS_2-G normalized to the EASA before and after NaOH treatment in 0.5 M Na_2SO_4 solution. Scan rate: 10 mV s^{-1}.

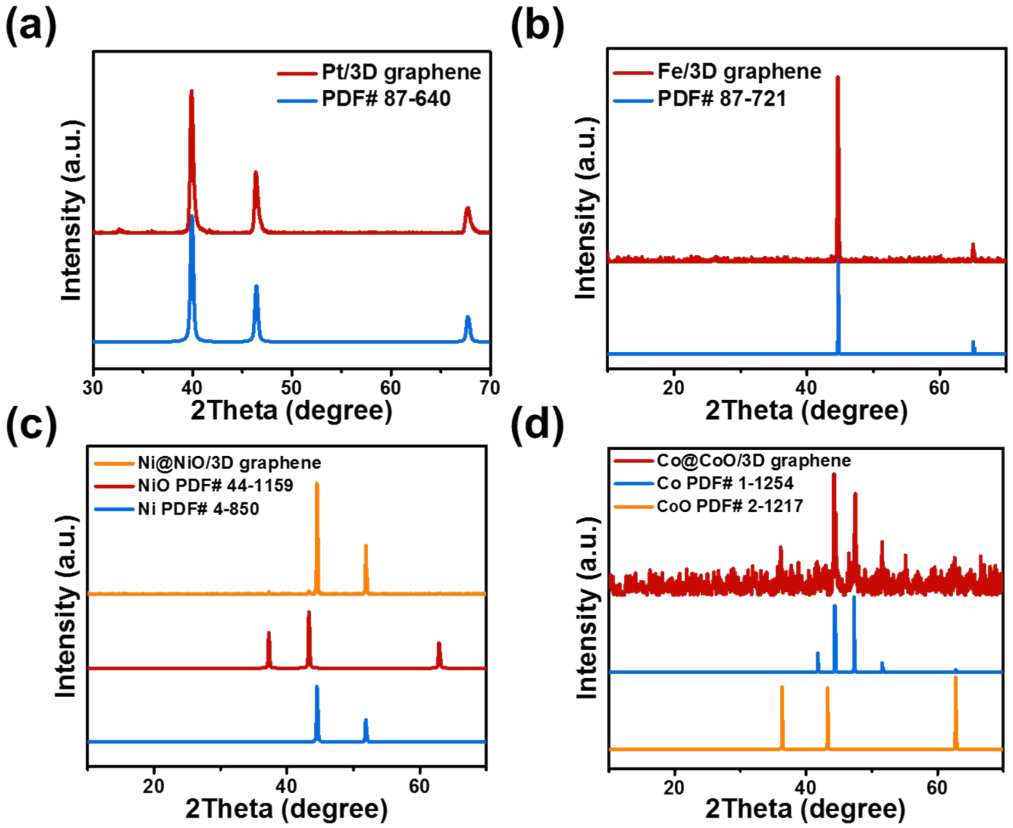

Figure S8. The XRD patterns of (a) Pt-G, (b) Fe-G, (c) Ni@NiO-G and (d) Co@CoO-G samples.

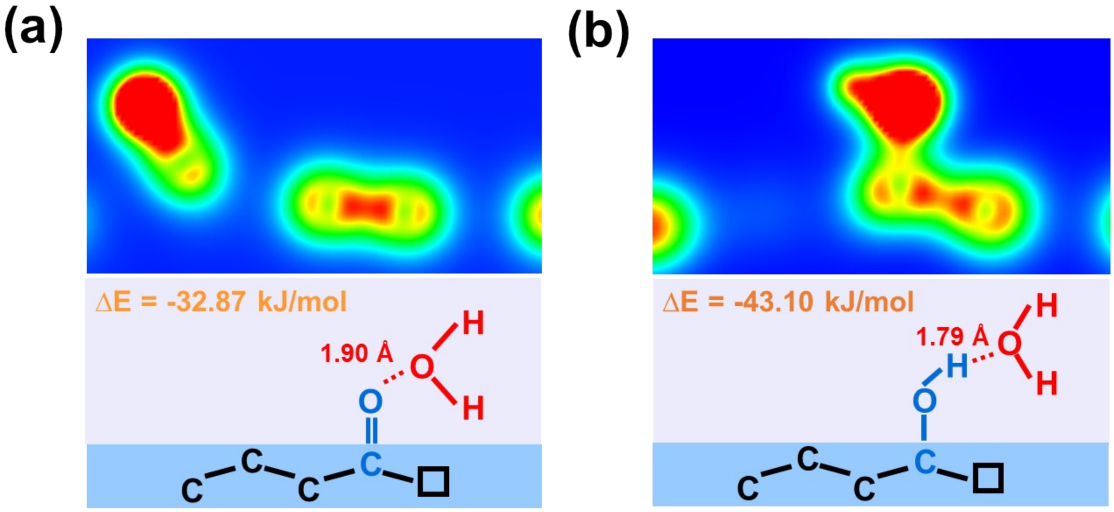

Figure S9. (a) Charge density contour plot (topside) of G-vac-O and corresponding water adsorption optimized configuration (downside). (b) Charge density contour plot (topside) of G-vac-OH and corresponding water adsorption optimized configuration (downside).

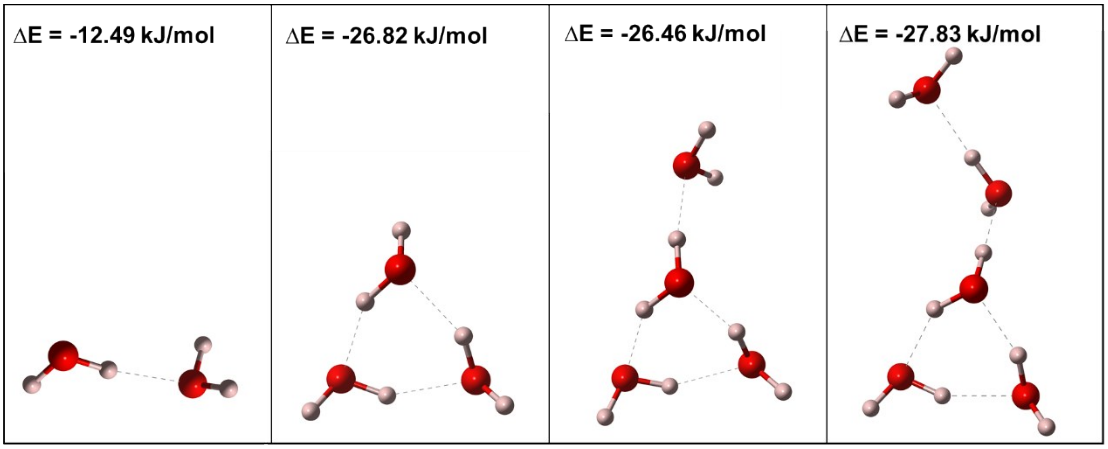

Figure S10. Optimized configurations and binding energies of water clusters with different number of water molecules.

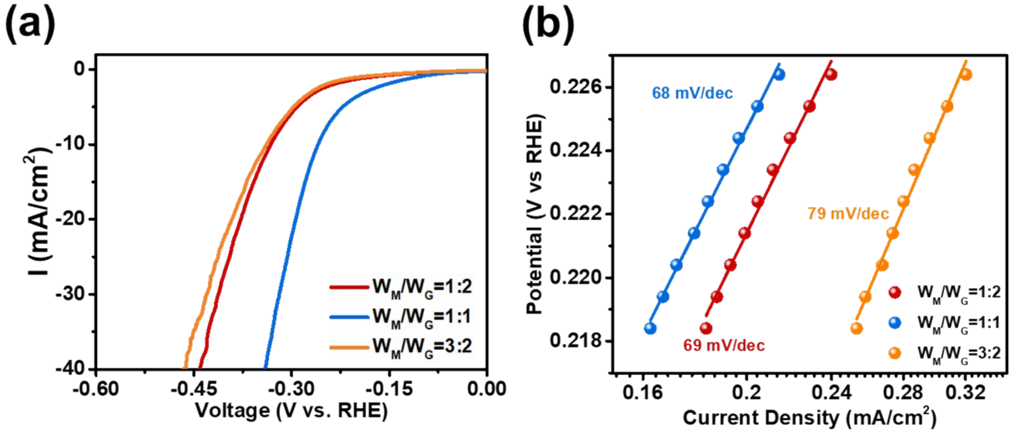

Figure S11. a) LSV curves and b) Tafel plots curves of MoS_2/graphene structures prepared by adding different mass ratio of W_{ATTM}:$W_{Glucose}$ = 1:2, W_{ATTM}:$W_{Glucose}$ = 1:1 and W_{ATTM}:$W_{Glucose}$ = 3:2, respectively, in 1.0 M NaOH solution.

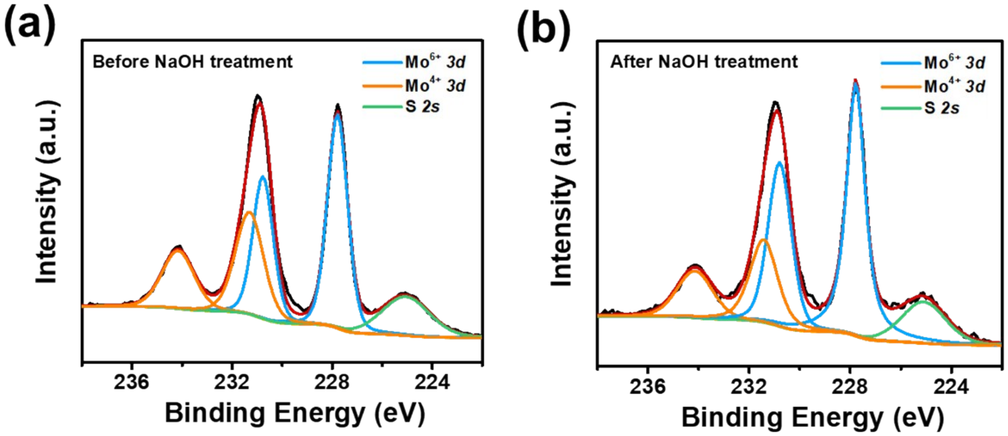

Figure S12. Chemical composition analysis by XPS for Mo in MoS2-G sample (a) before and (b) after 8-hour NaOH treatment.

Table S1. Comparison of HER performance of various Mo-based electrocatalysts in alkaline medium.

	Onset Potential (1mA/cm^2)	**Tafel Slope**	**Reference**
Mo_2C	≈ 135 mV	54 mV/dec	[4]
MoS_2/graphene/Ni foam	≈ 300 mV	98 mV/dec	[5]
$CoMoS_x$	≈ 120 mV		[6]
MoS_2/Mo	≈ 80 mV	87 mV/dec	[7]
MoS_2/Carbon Cloth	≈ 70 mV	156.7 mV/dec	[8]
NiS_2/MoS_2	76 mV	70 mV/dec	[9]
MoS_2/Ti	≈ 70 mV	100 mV/dec	[10]
MoS_2@MoP	42 mV		[11]
Ni doped MoS_2	45 mV	60 mV/dec	[12]
MoS_2/Ni_3S_2/Ni Foam	≈ 30 mV	61 mV/dec	[13]
This Work	60 mV	70 mV/dec	

References

1. J. P. Perdew, K. Burke and M. Ernzerhof, *Phys. Rev. Lett.*, 1996, **77**, 3865.

2. T. Bučko, J. Hafner, S. Lebègue and J. G. Ángyán, *J. Phys. Chem. A*, 2010, **114**, 11814.

3. S. Meng, E. G. Wang and S. W. Gao, *Phys. Rev. B*, 2004, **69**, 195404.

4. H. Vrubel and X. L. Hu, *Angew. Chem.* 2012, **124**, 12875.

5. X. Geng, W. Wu, N. Li, W. Sun, J. Armstrong, A. Al-hilo, M. Brozak, J. Cui and T. -p. Chen, *Adv. Funct. Mater.*, 2014, **24**, 6123.

6. J. Staszak-Jirkovský, C. D. Malliakas, P. P. Lopes, N. Danilovic, S. S. Kota, K. -C. Chang, B. Genorio, D. Strmcnik, V. R. Stamenkovic, M. G. Kanatzidis and N. M. Markovic, *Nat. Mater.* 2016, **15**, 197.

7. Z. H. Pu, Q. Liu, A. M. Asiri, Y. L. Luo, X. P. Sun and Y. Q. He, *Electrochimica. Acta.*, 2015, **168**, 133.

8. W. X. Zhu, C. Tang, D. N. Liu, J. L. Wang, A. M. Asiric and X. P. Sun, *J. Mater. Chem. A*, 2016, **4**, 7169.

9. T. C. An, Y. Wang, J. Tang, W. Wei, X. Q. Cui, A. M. Alenizi, L. J. Zhang and G. F. Zheng, *J. Mater. Chem. A*, 2016, **4**, 13439.

10. J. L. Shi and J. M. Hu, *Electrochimica. Acta.*, 2015, **168**, 256.

11. A. P. Wu, C. G. Tian, H. J. Yan, Y. Q. Jiao, Q. Yan, G. Y. Yang and H. G. Fu, *Nanoscale*, 2016, **8**, 11052.

12. J. Zhang, T. Wang, P. Liu, S. H. Liu, R. H. Dong, X. D. Zhuang, M. W. Chen and X. L. Feng, *Energy Environ. Sci.*, 2016, **9**, 2789.

13. Y. Q. Yang, K. Zhang, H. L. Lin, X. Li, H. C. Chan, L. C. Yang and Q. S. Gao, *ACS Catal.* 2017, **7**, 2357